Agricultural and Forest Meteorology, 67 (1994) 269–290

0168-1923/94/$07.00

Applying an empirical model of stomatal conductance to three C-4 grasses

Robert L. Dougherty[a], James A. Bradford[a], Patrick I. Coyne[b], Phillip L. Sims*[,a]

[a]*Southern Plains Range Research Station, USDA-ARS, 2000 18th Street, Woodward, OK 73801, USA*
[b]*Kansas Agricultural Experiment Station, Hayes, KS 67601, USA*

(Received 9 November 1992; revision accepted 8 July 1993)

Abstract

An empirical equation for stomatal conductance has been developed. The equation is based on a linear index, which was modified to represent nonlinear independent effects of CO_2 flux and water vapor pressure deficit. The equation was applied to data from caucasian bluestem (*Bothriochloa caucasia* (Trin.) C.E. Hubb.) and two accessions of Eastern gamagrass (*Tripsacum dactyloides* (L.) L.), measuring responses of leaves of the three grasses to wide ranges of environmental conditions. The equation accurately predicts stomatal conductance in these C-4 grasses, but requires measured photosynthesis as an input variable. Dependence on only environmental inputs was achieved by including the equation as the conductance submodel in a complete leaf gas exchange model, along with a photosynthesis submodel derived from a biochemically based model. This simplified submodel also describes the data well, as does the integrated model. Comparisons of model results and derived parameter values indicate important differences among gas exchange properties of the three grasses. Implementation details of the model are discussed, along with approaches for adapting it for simulating interleaf variability, water stress effects, and patchy stomatal function.

1. Introduction

In arid and semiarid environments, the regulation of water loss is among the most important processes determining the success of plant species. Stomata are generally recognized as the principal regulators of water loss through leaves, but they also affect the exchange of carbon dioxide between the mesophyll and the atmosphere. Most simulation models of plant function that are intended to describe interactions between carbon fixation and transpiration use a stomatal component to calculate both transpiration and the supply of CO_2 within the leaf air space. However, the physiological mechanisms of stomatal movement are incompletely understood, and empirical models are still necessary to predict stomatal response to environmental

* Corresponding author.

SSDI 0168-1923(93)02096-O

variables (Collatz et al., 1991). Current empirical models differ in their formulation of stomatal responses to the environmental variables that also directly affect photosynthesis, namely, radiation, CO_2 and temperature. Several stomatal models include functional responses to these variables (Jarvis, 1976; Bakker, 1991), while others explicitly include a photosynthesis term and a correlation of stomatal conductance with photosynthesis (Farquhar and Wong, 1984; Collatz et al., 1991). The latter approach seems more valuable both in theory and application: it embodies the hypothesis that stomatal aperture is regulated by photosynthetic electron transport in the guard cells, and it allows a stomatal submodel to shift the burden of calculating the highly nonlinear effects of light, temperature and, to some extent, CO_2, to a separate photosynthesis submodel. This approach makes the simplifying assumption that guard cell electron transport and mesophyll carbon fixation respond similarly to similar conditions. While guard cell and mesophyll responses can be experimentally decoupled, for example with blue light (Karlsson and Assman, 1990), much evidence suggests parallel responses under most conditions (Wong et al., 1979; Bunce, 1987; Radin et al., 1988). The use of a photosynthesis submodel, calibrated for mesophyll responses, to represent guard electron transport thus allows a relatively simple model to describe this complex system.

In this paper, we test the empirical stomatal submodel of Ball (1988; Collatz et al., 1991) with gas exchange data for three C-4 grass varieties comprising two species. We extend the submodel to describe responses to conditions beyond those investigated in previous studies, and link it with an empirical photosynthesis submodel. We then test the integrated model with an independent data set for one of the grasses. The extended stomatal submodel, and the integrated model, provide the opportunity to compare gas exchange responses of several species by evaluating a small number of parameters.

2. Gas exchange data

We developed the stomatal submodel using gas exchange data for caucasian bluestem accession WW-765 (*Bothriochloa caucasia* (Trin.) C.E. Hubb) and two accessions of Eastern gamagrass (*Tripsacum dactyloides* (L.) L.): WW-1318, a relatively narrow leafed variety from Texas, and WW-1462, a wider leafed grass from Missouri. Results and analyses of caucasian bluestem and eastern gamagrass gas exchange experiments were published by Coyne and Bradford (1983, 1985). In the current study, these data were used to compare various stomatal submodel formulations, to identify differences in conductance responses among grass varieties, and to test the stomatal submodel in the context of a complete leaf gas exchange model. Model predictions for caucasian bluestem were then compared with measurements from data collected in a separate study (Coyne et al., 1982).

2.1. Plant culture

Plants were transplanted from the field into 18 dm^3 drained plastic buckets and grown in a greenhouse. Soil water was maintained at or near field capacity and fertility was optimized with periodic additions of nutrient solution. Supplemental lighting (400 W high pressure sodium lamps) was used to achieve a 14 h photoperiod. Photosynthetic flux density (Q_p; see Appendix 1 for list of symbols) in the absence of sunlight was about 700 $\mu mol\ m^{-2}\ s^{-1}$ at 1 m above the soil surface. Sunlight plus the supplemental lighting produced Q_p levels higher than 2000 $\mu mol\ m^{-2}\ s^{-1}$ at midday. Daytime temperatures varied from 25 to 35°C and night-time temperatures averaged near 25°C.

2.2. Leaf gas exchange

The exchange of CO_2 and water vapor of individual leaves, representing the population of youngest, fully expanded lamina, was measured in a steady state, temperature controlled chamber. Response of gas exchange to light, temperature, ambient water vapor density gradient (D_a), and ambient CO_2 concentration (c_a) was determined by varying one and holding the other variables approximately constant. Discrete light levels were achieved by varying the height of a 1000 W multivapor lamp mounted in a parabolic reflector. The caucasian bluestem data used in the present study for model validation were measured at near-saturating irradiance only. Temperature was controlled by thermoelectric modules.

3. Stomatal submodel

3.1. Submodel development and application to caucasian bluestem and eastern gamagrass

The equation of Ball (1988; Collatz et al., 1991) uses a single empirical index that combines the influences of three variables on stomatal conductance to water vapor (g_s, mol $m^{-2}\ s^{-1}$): net CO_2 assimilation (A_n, mol $CO_2\ m^{-2}\ s^{-1}$), leaf surface relative humidity (h_S, dimensionless fraction), and leaf surface CO_2 mole fraction (c_S, dimensionless fraction)

$$g_S = b_0 + b_1 \frac{A_n h_s}{c_S} \tag{1}$$

The variables used in this and subsequent indices were chosen based both on their predictive utility and their general availability in most field and laboratory gas exchange measurements.

Leuning (1990) adjusted the value of c_S in Eq. (1) by subtracting $\Gamma(CO_2$

compensation mole fraction); however, for the C-4 grasses considered here, Γ is too low (0–10, μmol mol^{-1}) for this adjustment to improve the predictive power of Eq. (1) or other stomatal equations developed in this paper.

Mott and Parkhurst (1991) and Aphalo and Jarvis (1991) argued that stomata respond not to h_S, but to vapor pressure deficit. To evaluate whether the stomatal index could be improved by including such a response, we modified Eq. (1) to use vapor pressure deficit at the leaf surface, D_S (kPa)

$$g_S = b_0 + b_1 \frac{A_n}{D_S c_S} \tag{2}$$

The empirical terms b_0 and b_1 in Eqs. (1) and (2) are determined for a given species by regression using leaf gas exchange measurements made under a number of conditions of light, CO_2 mole fraction, temperature and humidity. D_S, h_S and c_S can be calculated from ambient and leaf internal conditions using standard gas exchange equations (Ball, 1987; Field et al., 1989).

We compared the measured conductances to values of the indices from Eqs. (1) and (2). Examination of the plots of g_S vs. these stomatal indices (Fig. 1) suggests several conclusions:

1. There is much scatter in the relationship between g_S and the stomatal index of Eq. (1) (Fig. 1(a)). The stomatal index based on vapor pressure deficit

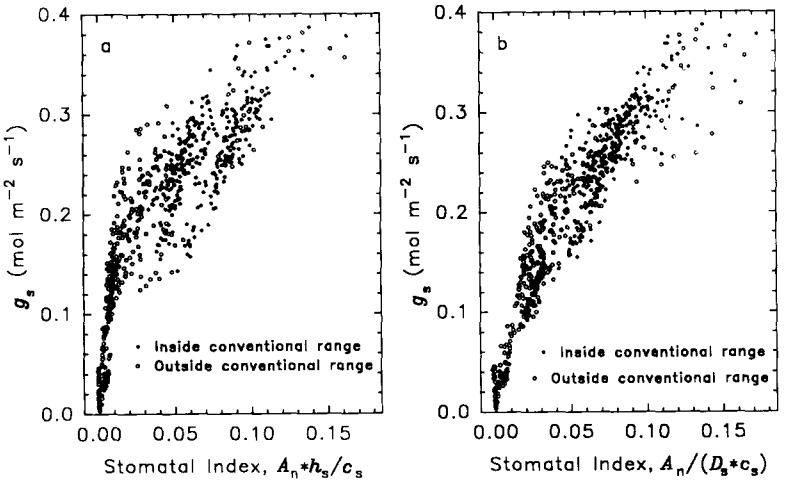

Fig. 1. Stomatal conductance of caucasian bluestem, plotted against (a) the stomatal index of Eq. (1), based on relative humidity, and (b) the stomatal index of Eq. (2), based on vapor pressure deficit. Closed circles: observations within the ranges used by Collatz et al. (1991): T_l (leaf temperature) = 20–35°C, Q_p (Irradiance) > 0.0001 mol m^{-2} s^{-1}, 0.45 < h_S < 0.90, and c_S > 0.0001 mol mol^{-1}. Open circles: measurements at temperatures as low as 15°C and as high as 45°C, Q_p as low as 0 μmol m^{-2} s^{-1}, and h_S as low as 0.14.

(Eq. (2)) shows a closer correspondence to measured conductance, but some scatter remains (Fig. 1(b)).

2. Within the ranges of environmental variables reported by Collatz et al. (1991), the relationships between g_S and the indices appear relatively linear, but the more extreme environmental conditions included here impart curvature to the relationships.

3. Cases where $A_n < 0$ because of very low Q_p result in small negative values of the stomatal indices, which still conform to the overall nonlinear relationships. This suggests the value of using an empirical stomatal equation for simulating night-time conductances.

To develop an empirical stomatal submodel applicable to a relatively wide range of conditions, we considered four nonlinear equations. Among the simplest forms are the power functions, employing either humidity or vapor pressure deficit

$$g_S = b_0 \left[\frac{A_n h_S}{c_S}\right]^{b_1} \tag{3}$$

and

$$g_S = b_0 \left[\frac{A_n}{D_S c_S}\right]^{b_1} \tag{4}$$

Equations (1)–(4) imply that the effects of A_n, c_S, and h_S or D_S on stomatal conductance are compensatory. For example, a 50% increase in A_n has the same effects in these equations as a 50% increase in h_S or a 33% decrease in D_S or c_S. These compensatory relationships, while plausible for restricted ranges of environmental conditions, may not apply to the wide range of data considered here. We extended Eqs. (3) and (4) further by considering separate multiplicative terms for carbon and humidity

$$g_S = b_0 \left[\frac{A_n}{c_S}\right]^{b_1} h_S^{b_2} \tag{5}$$

$$g_S = b_0 \left[\frac{A_n}{c_S}\right]^{b_1} \frac{1}{D_S^{b_2}} \tag{6}$$

Other equations that included separate statistical terms for A_n and c_S, while more complex than the above equations, did not provide improved fits to the data.

We evaluated Eqs. (1)–(6) using linear regression; variables in the nonlinear equations were first transformed to forms linear in the parameters (Draper and Smith, 1981). For numerical reasons, regression analyses did not include cases where $A_n \leqslant 0$. However, these cases were included in subsequent

Table 1
Coefficients of determination for six stomatal submodel formulations, applied to three grasses. Equation numbers correspond to those in the text. See Appendix 1 for definitions of terms

#	Equation: $g_s =$	r^2		
		Caucasian Bluestem	Eastern Gamagrass	
			WW-1318	WW-1462
		($n = 692$)	($n = 430$)	($n = 422$)
1	$b_0 + b_1 \frac{A_n h_S}{c_S}$	0.75	0.71	0.75
2	$b_0 + b_1 \frac{A_n}{D_S c_S}$	0.83	0.78	0.76
3	$b_0 \left[\frac{A_n h_S}{c_S}\right]^{b_1}$	0.77	0.82	0.82
4	$b_0 \left[\frac{A_n}{D_S c_S}\right]^{b_1}$	0.89	0.88	0.88
5	$b_0 \left[\frac{A_n}{c_S}\right]^{b_1} h_S^{b_2}$	0.85	0.88	0.92
6	$b_0 \left[\frac{A_n}{c_S}\right]^{b_1} \frac{1}{D_S^{b_2}}$	0.91	0.91	0.94

applications of the integrated leaf gas exchange model, as explained later. We analyzed the six equations using measurements of leaf gas exchange for caucasian bluestem (Coyne and Bradford, 1983) and two accessions of eastern gamagrass (Coyne and Bradford, 1985). Data from all four manipulations ($Q_p \times T_l$, $e_a \times T_l$, $c_a \times T_l$ and T_l alone) in these experiments were used in the submodel comparisons. To clarify the relative merits of D_S and h_S for predicting g_S, we calculated additional regression analyses using only data from the $e_a \times T_l$ manipulations. Conformance of the various models to the data was evaluated using the coefficient of determination, r^2 (Table 1).

As proposed above, the nonlinear forms of the simple univariate equations fit the leaf gas exchange data better than did the linear forms (i.e. r^2 values for Eqs. (3) and (4) exceed those for Eqs. (1) and (2), respectively, see Table 1). Extending the simple nonlinear forms by separating effects of carbon flux and humidity also resulted in improved fit to the data. The findings of Aphalo and Jarvis (1991) are supported, in that each of the three equations that used D_S was better correlated with g_S than the analogous equation based on h_S (Table 1). Similar comparisons among regressions resulted from analyses restricted to data from the $e_a \times T_l$ experiments (results not shown).

We consider Eq. (6) to be the most appropriate empirical submodel for these three C-4 grasses. This equation explains more of the variation in stomatal conductance than the other equations.

3.2. Comparison of stomatal properties among grasses

Parameter values for Eq. (6) were determined for the three grasses using nonlinear regression. Parameter values show large differences among grasses (Table 2). The two gamagrass accessions differ significantly ($P < 0.05$) in all three parameters.

The empirical parameters b_0, b_1 and b_2 in Eq. (6) represent, respectively, a scaling factor, the coupling of stomatal conductance to carbon flux, and stomatal response to humidity. Differences among grasses in the parameter b_0 reflect differences in the overall stomatal response to changes in both carbon and humidity. Separate submodel analyses (not shown) in which b_0 was held to a constant value for all three grasses resulted in values of b_1 and b_2 that compare similarly to those in Table 2.

Differences among grasses in the parameter b_1 reflect differences in coupling of stomatal conductance to carbon assimilation. Calculations of estimated conductance at two values of A_n for the three grasses show that high values of b_1 result in large declines in stomatal conductance as the ratio A_n/c_S decreases (Table 2). Of the three grasses analyzed, the two eastern gamagrass accessions WW-1318 and WW-1462, respectively, showed the smallest and the largest degree of coupling of conductance to carbon flux (Table 2).

The parameter b_2 represents the degree of stomatal response to humidity. Calculations of estimated stomatal conductance at two humidity levels show that high values of b_2 result in large declines in conductance as D_S increases (Table 2). According to these calculations, the two eastern gamagrass accessions display less of a stomatal response to humidity than does the bluestem.

The preceding analyses of the stomatal submodel are incomplete because they assume a stomatal response to A_n. However, stomata actually influence A_n by regulating c_i. A more complete analysis of stomatal response to the

Table 2
Stomatal conductance submodel parameters and calculated conductances for three grasses. Parameter values b_0, b_1 and b_2 are the estimated parameter values of Eq. (6), determined by multiple regression. Parameter estimates within a column not followed by common letters are significantly different ($P < 0.05$). Estimates of stomatal conductance ($\hat{g}_S$ mol m^{-2} s^{-1}) for the three grasses were calculated under three conditions of A_n (μmol m^{-2} s^{-1}), c_S (μmol mol^{-1}), and D_S (kPa)

Variety	b_0	b_1	b_2	$\hat{g}_S$ ($A_n = 30$; $c_S = 320$; $D_S = 1$)	$\hat{g}_S$ ($A_n = 10$; $c_S = 320$; $D_S = 1$)	$\hat{g}_S$ ($A_n = 30$; $c_S = 320$; $D_S = 6$)
Caucasian bluestem	1.18 a	0.618 a	0.339 a	0.274	0.139	0.149
Eastern gamagrass:						
WW-1318	1.17 a	0.541 b	0.298 a	0.324	0.179	0.190
WW-1462	1.45 b	0.663 a	0.235 b	0.301	0.145	0.198

environment requires the stomatal submodel to be integrated with a photosynthesis submodel.

4. Implementation in a leaf gas exchange model

4.1. Development of a photosynthesis submodel

We constructed an empirical submodel for C-4 photosynthesis by simplifying the C3 model of Farquhar et al. (1980). Several terms representing processes that are relatively unimportant in C-4 photosynthesis were removed. As in the model of Farquhar et al. (1980), A_n was estimated as the minimum of two photosynthetic capacities, here termed A_1 and A_2. A_1 was limited by radiation and a maximum photosynthetic flux (A_m, mol CO_2 m^{-2} s^{-1}), and was modeled with the nonrectangular hyperbola of Prioul and Chartier (1977)

$$A_1 = \frac{A_m + \alpha Q_p \sqrt[2]{A_m^2 - 2A_m \alpha Q_p \cdot (2\theta - 1) + \alpha^2 Q_p^2}}{2\theta} \tag{7}$$

Here, α is an empirical parameter representing quantum efficiency (mol CO_2 mol^{-1} incident photons) and θ is an empirical shape parameter determining the smoothness of the transition between limitation by Q_p and by A_m (Prioul and Chartier, 1977). Equation (7) is identical to the Farquhar et al. (1984) equation for light limited photosynthetic capacity, once the assumption is made that Γ^* (CO_2 compensation concentration, ignoring mitochondrial respiration) is negligible.

A_2 was limited by c_i and A_m, and is analogous to the rubisco limited photosynthesis of Farquhar et al. (1980), again assuming a negligible Γ^*

$$A_2 = A_m \frac{c_i}{c_i + \frac{1}{E_c}} \tag{8}$$

The parameter E_c is a dimensionless, empirical index of the leaf's CO_2 efficiency (Van Bavel, 1975). Net photosynthesis was modeled as a minimum of A_1 and A_2, less dark respiration (R_d, mol CO_2 m^{-2} s^{-1})

$$A_n = \min(A_1, A_2) - R_d \tag{9}$$

Temperature dependence of maximum photosynthesis was simulated using an Arrhenius function (Feng et al., 1990)

$$A_m = \frac{\exp\left(K_a - \frac{E_a}{RT_k}\right)}{1 + \frac{E_a}{dH - E_a} \exp\left(\frac{dH}{RT_o} - \frac{dH}{RT_k}\right)} \tag{10}$$

where K_a, E_a and dH are empirical parameters, T_k is leaf temperature (K), R is the gas constant, and T_o is the temperature at which A_m is maximized (K).

The photosynthesis submodel, complete with temperature dependency, has eight adjustable parameters, roughly half the number of more detailed models (e.g. Collatz et al., 1991). Inclusion of Γ^*, temperature dependencies of R_d, and smoothing of the minimum function in Eq. (9) resulted in no improvement of model performance. Our objective was to develop as simple a photosynthesis model as would adequately describe the data, in order to analyze further the stomatal submodel. Therefore, the simplified photosynthesis submodel was used for all subsequent analyses. Use of a more complex set of equations may be appropriate in certain situations, but would not be expected to change the results of the present analyses.

Parameter values were determined for caucasian bluestem and the two gamagrass accessions. We estimated T_o from graphs of the data. The other seven parameters (K_a E_a, dH, α, θ, E_c and R_d) were estimated using nonlinear regression.

Large differences in parameter values were found among the three grasses (Table 3). Of the three, caucasian bluestem was found to have the lowest maximum photosynthetic rate and the smallest photon flux and CO_2 efficiencies. Of the gamagrasses, accession 1462 had the higher maximum photosynthetic rate and photon flux and CO_2 efficiencies.

4.2. Integration of stomatal and photosynthesis submodels

In order to simulate leaf responses to environmental variables, separate submodels for g_S and A_n must be solved simultaneously (Tenhunen and

Table 3
Photosynthesis submodel parameters and calculations for three grasses. See text for explanation of parameters. A_m @ T_o is the maximum photosynthetic rate (mmol m^{-2} s^{-1}) calculated from Eq. (11) using the first four parameters values in the appropriate column of this table. Relative Absolute Mean Error (RAME) is a goodness-of-fit statistic (Appendix 2); a low value indicates that the model fits the data well

Value	Caucasian bluestem	Eastern gamagrass	
		WW-1318	WW-1462
T_o(°C)	34	36	36
K_a	28.6	16.3	16.3
E_a	61960	31040	30500
dH	173300	288000	265200
α	0.065	0.112	0.155
θ	0.936	0.666	0.632
E_c	0.053	0.067	0.073
R_d	1.21	4.13	4.58
A_m @ T_o	47.7	62.3	75.8
RAME (%)	13.9	11.4	9.3

Westin, 1979). We linked the submodels by using a diffusion equation for c_i

$$c_i = c_S - 1.6\frac{A_n}{g_S} \tag{11}$$

where 1.6 is the ratio of the diffusivities of water vapor and CO_2 in air. To implement the complete leaf gas exchange model, a numerical algorithm was used to determine values of c_i and g_S which satisfy Eqs. (6), (9), and (11). We tested this solution with wide ranges of environmental conditions. The algorithm found unique values of c_i and g_S for all conditions except extremely low levels of D_S or c_S, and when $A_n \leqslant 0$ (i.e. net respiration). Keeping D_S, c_S, and g_S at or above the minimum values of 1 kPa, 50 μmol mol^{-1}, and 0.01 mol m^{-2} s^{-1}, respectively, allowed the algorithm to perform satisfactorily under all tested conditions.

4.3. Application of integrated gas exchange model to three grasses

We applied the integrated model to the leaf gas exchange data used to

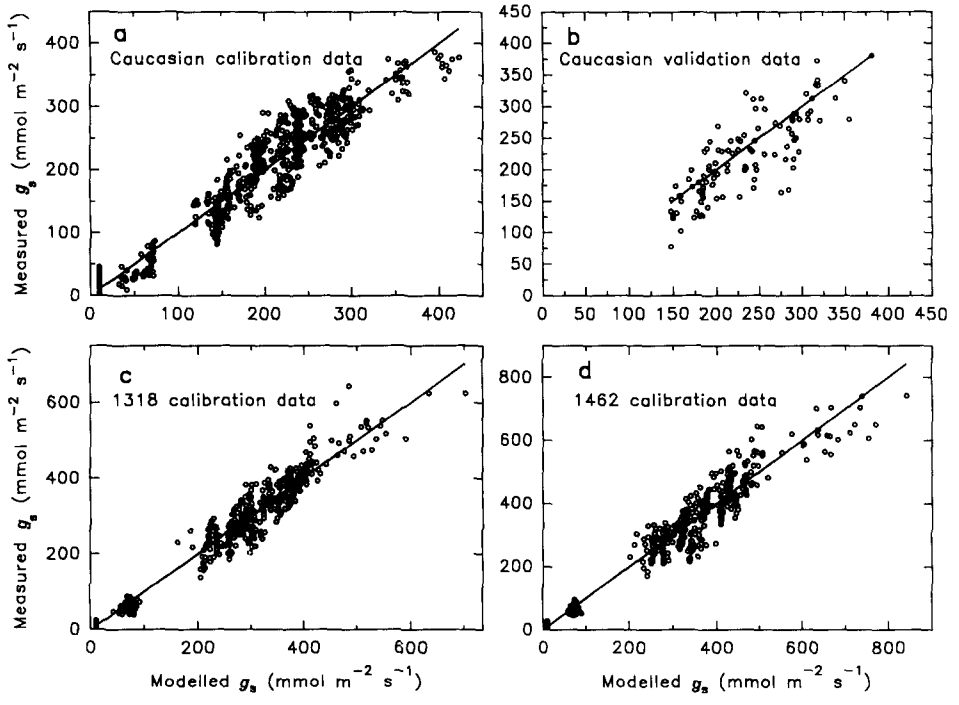

Fig. 2. Measured (symbols) stomatal conductance, plotted against simulated values for four datasets: (a) caucasian bluestem calibration data; (b) caucasian bluestem independent dataset; (c) eastern gamagrass accession WW1318; (d) eastern gamagrass accession WW-1462. Lines represent the expected Observed = Simulated relationships.

Table 4
Relative Absolute Mean Errors for the integrated leaf gas exchange model and its component submodels. Conductance and photosynthesis submodels were calibrated for each of three grasses, and simulations were run first for the separate submodels and then for the integrated model. Simulations included runs using the data used to calibrate the submodels, as well as a single validation dataset for caucasian bluestem

Model	Dependent variable	RAME (%)			
		Calibration data			Validation data
		Caucasian bluestem	Eastern gamagrass		Caucasian bluestem
			WW-1318	WW-1462	
g_s submodel	g_s	9.5	9.3	9.9	10.9
	E	9.5	9.3	9.1	9.9
A_n submodel	A_n	14.0	11.7	9.5	22.4
Integrated	g_s	12.7	9.4	10.9	13.9
	E	12.5	9.5	10.1	14.2
	A_n	10.6	9.6	8.3	15.5

calibrate the submodels for the three grasses. An independent data set for caucasian bluestem was also used and is discussed in a later section. For each grass, we set the 12 adjustable parameters to the values determined for that grass. We then applied the model to the environmental variables (Q_p, T_l, e_S, and c_a) measured with each observation of leaf gas exchange for that grass. A_n and g_S were calculated as described above, and transpiration (E, mol m^{-2} s^{-1}) was calculated from the conductances and water vapor pressures (Pearcy et al., 1989). Calculated values of A_n, g_S, and E were compared with measured values. Analyses included all measurements where $c_a > 20$ μmol mol^{-1}. Goodness of fit was evaluated using model residuals expressed as Relative Absolute Mean Errors (RAME; see Appendix 2).

Calculated photosynthesis rate, stomatal conductance and transpiration rate were close to the observed calibration values for the three accessions (Fig. 2(a), (c), (d)). Relative residuals calculated using calibration data for A_n, g_S and E using the integrated model were 13% or less (Table 4). Model performance with an independent data set (Fig. 2(b)) is discussed in a later section.

Performance of the integrated model can be evaluated with graphs of observed and simulated results against controlled environmental variables. Graphs were constructed showing these responses for one species, caucasian bluestem, using the dataset used to calibrate the model (Fig. 3). Measured and simulated A_n, g_S and E are in close agreement at all levels of the light and CO_2 experiments, and at temperatures up to 35°C in the temperature experiment. Discrepancies occur at higher temperatures, because model fitting was not greatly influenced by the small number of measurements above 35°C. Also,

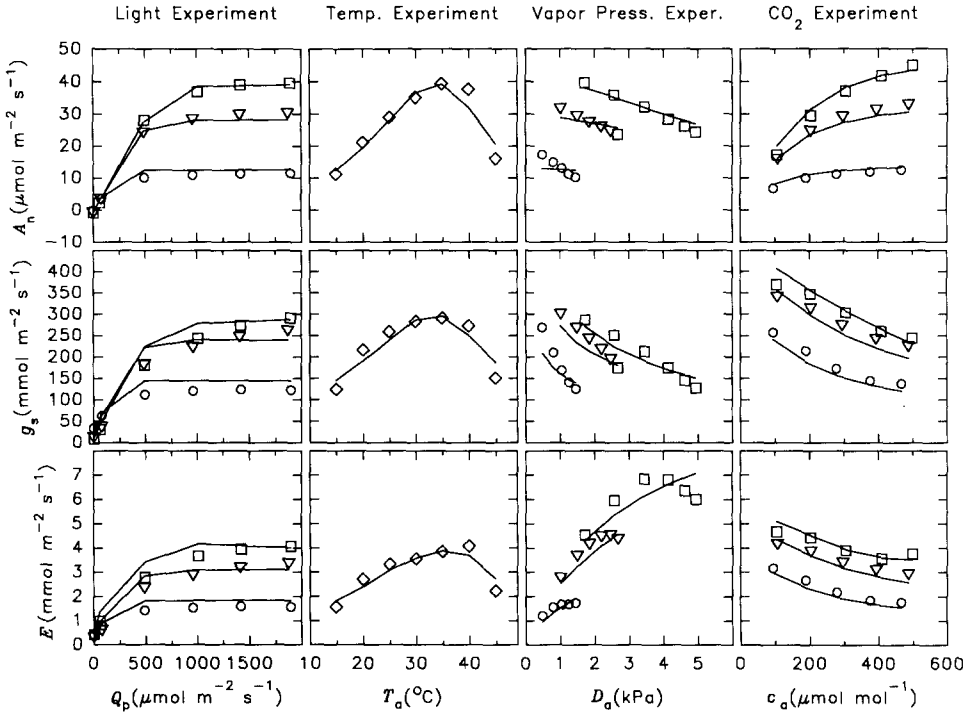

Fig. 3. Observed (symbols) and simulated (lines) responses of photosynthesis, stomatal conductance, and transpiration to four environmental variables, for caucasian bluestem. Each column of scatter plots (except for the temperature experiment) shows results for experiments in which one environmental variable was varied at three temperatures. Leaf temperatures in those columns of scatterplots are indicated by symbols (circles: 15°C; triangles: 25°; squares: 35°). Each symbol represents the average values for 9–20 observations within a treatment group.

in the vapor pressure experiment, simulated A_n and g_S do not display the degree of responsiveness to D_a seen in the observed data. Model analysis indicates that this is caused by the photosynthesis submodel's lack of a response to humidity, except indirectly through the effect on conductance. Generally, the integrated model produced fits better to the photosynthesis data, and worse to the conductance and transpiration data, than did the component submodels tested alone (Table 4). This may reflect a large degree of error in measurements of c_i in the original data. Measured values of c_i were used in testing the photosynthesis submodel, but c_i was itself simulated in the integrated model.

4.4. Error analysis of integrated model

We carried out an error analysis on model results for caucasian bluestem, to evaluate the effects of experimental conditions on model performance. We

first calculated residuals from log-transformed observed and simulated values of g_S and A_n. This reduced heterogeneity of the residuals' variances across treatments; however, cases where $A_n \leqslant 0$ had to be excluded from this analysis. The residuals were tested with analysis of variance, using primary experimental treatment and leaf replicate as independent effects, and residuals for g_S and A_n as separate dependent variables. The analysis was repeated for each of the four experiments and each of the three temperatures, except when temperature itself was the primary experimental treatment. This reflects the design of the original experiments (Coyne and Bradford, 1983, 1985) where each leaf replicate was subjected to a range of a single environmental variable. Results of this analysis reveal that variation among individual leaves accounts for the greatest share of the model error: leaf replicate was significantly associated with errors in predicted g_S and A_n in all experiments and temperature levels ($P < 0.01$). Primary treatment level was also significantly associated with model errors ($P < 0.01$), except for the leaves measured at 15°C in the light and CO_2 experiments. Model goodness-of-fit clearly varied across treatment gradients, as suggested by Fig. 3. However, the error analysis reveals that variability of model errors, probably resulting from physiological differences between leaves, are even greater than these treatment differences.

4.5. Application of integrated model to an independent data set

The model was applied to leaf gas exchange data for caucasian bluestem, collected in an independent study (Coyne et al., 1982). We used parameter values as calculated for caucasian bluestem in the analyses already discussed (Tables 2 and 3). The experiments used for validation differed from the ones in which parameters were calculated (i.e. calibration data) in the following aspects: (1) The validation study did not include manipulations of Q_p; (2) leaves in the validation study were exposed to a relatively narrow range of c_a treatments; (3) the D_a and c_a experiments in the validation study did not include 15°C temperature treatments; (4) fewer leaves were measured ($n = 130$).

Relative residuals from the validation data were higher than from the calibration data, and, as with the calibration simulations, the integrated model gave poorer fits to the conductance data and better fits to the photosynthesis data than did the standalone simulations with the submodels. Using the integrated model, the mean absolute residuals for conductance, transpiration and photosynthesis were within 16% of the average observed values (Table 4). The model showed a slight tendency to overestimate g_S in the validation dataset (Fig. 2(b)), an expected result, because observed fluxes in the validation data were also slightly lower than in the calibration data. The discrepancy in responses to D_a, noted earlier for the calibration simulations, also appeared in the validation results. However, as with the calibration

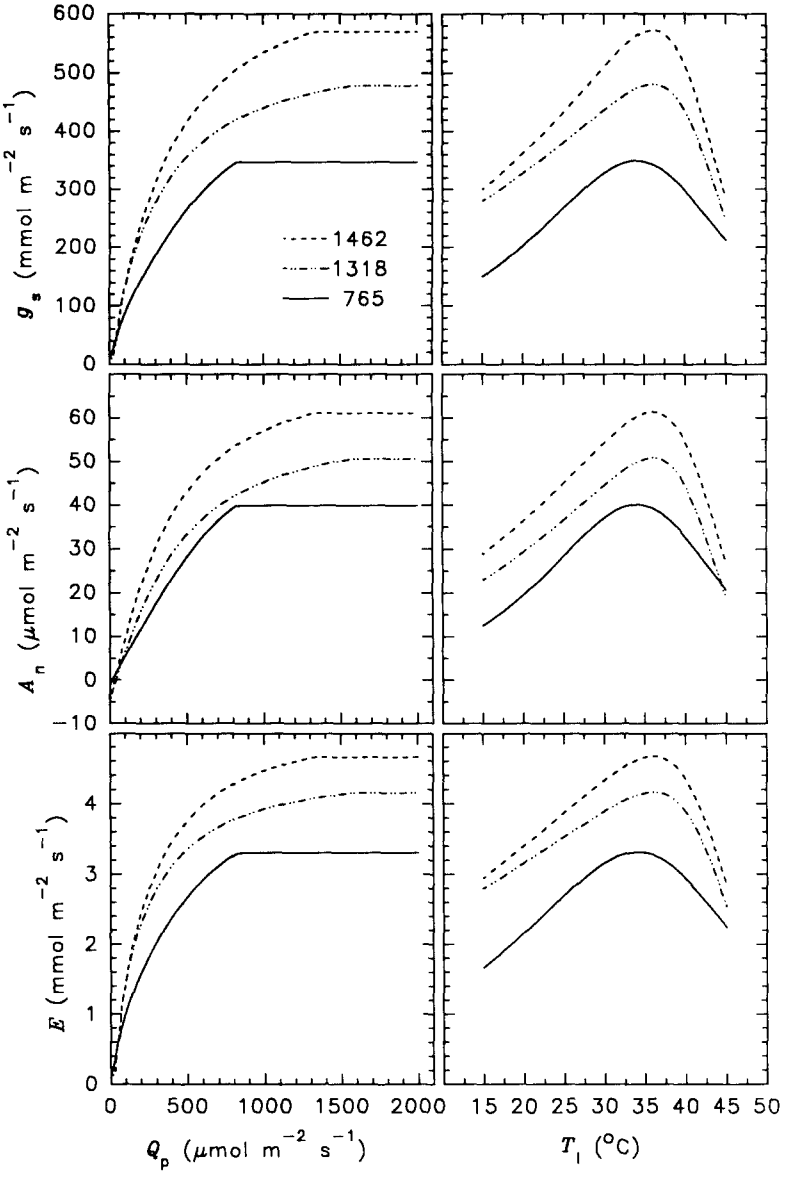

Fig. 4. Stomatal conductance, photosynthesis and transpiration of three grasses calculated with the integrated leaf gas exchange model across ranges of light and temperature. Each set of curves was generated by solving the integrated conductance and photosynthesis model across a single varying condition, while all other conditions were assumed constant. Constant environmental variables were: Q_p, 2000 μmol m^{-2} s^{-1}; c_a, 350 μmol mol^{-1}; T_l, 35°C; D_a, 1.3 kPa.

simulations, the greatest source of model error appeared to be leaf-to-leaf variation.

4.6. Comparing simulated gas exchange for three grasses

Figure 4 shows simulated g_S, A_n and E for the three grasses over ranges of Q_p and T_l similar to ranges in the calibration data. Simulated fluxes and conductance of eastern gamagrass accession 1462 exceed those of accession 1318; caucasian bluestem generally shows the lowest values. These curves reveal the effects of several important model parameters. Most obvious are the parameters K_a and E_a, which reflect the differences in photosynthetic capacities among the three grasses, and largely cause the different magnitudes of responses just noted. In addition, the distinct plateaus in caucasian bluestem's simulated responses to light are caused by the relatively high value of the θ parameter used for this grass. The effect of different optimal temperatures is seen in the temperature responses.

5. Discussion

5.1. Stomatal submodel

The application of the stomatal submodel of Ball (1988) and Collatz et al. (1991) to the data included in this study call into question that submodel's assumptions of linearity and the compensatory effects of carbon flux and humidity. The revised stomatal submodel developed here, and tested with C-4 grass data in the context of a complete leaf gas exchange model, does not contain these assumptions. The generally good fit of the revised submodel to these data has several implications for an increased understanding of stomatal behavior. First, the nonlinear relationship between g_S and A_n suggests that stomata are more sensitive to changes in environmental conditions when A_n is low than when A_n is high. This nonlinearity may be the effect of differential response of stomatal photosynthetic electron transport with respect to that of the mesophyll. Further study, involving the application of stomatal submodels to data collected under wide ranges of conditions, is necessary to determine whether these nonlinear relationships occur among other species.

Ball (1988) acknowledged the poor linearity between g_S and the stomatal index $A_n h_S / c_S$ at low photosynthesis and extreme humidities, and suggested the feasibility of constructing a nonlinear stomatal submodel. For his analyses, Ball (1988) considered the linear index to provide sufficient approximations of g_S, because of its simplicity and the fact that most of a plant's transpiration and photosynthesis tend to occur under conditions where the

linear index is applicable. However, the importance of early morning periods for gas exchange is greater for grasses in semiarid environments than for well-watered crops. As in Ball's (1988) analysis, when we applied Eq. (1) to leaves with relatively low A_n, using parameter values derived from measurements at higher A_n, that equation tended to underestimate g_S (see Fig. 1(a)). If a stomatal submodel based on Eq. (1) is used to simulate diurnal courses of gas exchange, the accumulated underestimation of g_S and E during periods of low light or high atmospheric water stress could lead to important errors in simulated water use.

The extended submodel, like the Ball (1988; Collatz et al., 1991) version, suggests that leaves 'sense', and respond to, CO_2 partial pressures and humidity within the leaf boundary layer, that is, at the leaf surface. Guard cells are thought to initiate these responses (Losch and Tenhunen, 1981). Recent work has challenged these assumptions. Mott (1988) suggested that stomata respond to c_i, rather than c_S. Other recent studies (Aphalo and Jarvis, 1991; Mott and Parkhurst, 1991) concluded that stomata respond to vapor pressure deficit, or the resulting transpiration stream, rather than relative humidity. The results of our study do not support a principal role of c_i in determining stomatal behavior; its use in place of c_S in the stomatal submodel did not improve the model's accuracy (results not shown). These results are not conclusive, being correlative rather than manipulative; also, estimates of c_i are subject to more error than are the values of c_S. However, our results do support the utility of c_S for predicting g_S. Regarding the choice of variables to account for the effect of humidity on g_S, our results indicate a greater utility of D_S than h_S. Using E in place of D_S did not improve the stomatal submodel (results not shown).

5.2. Integrated model

When the stomatal submodel was integrated with the photosynthesis submodel, the goodness-of-fit for g_S deteriorated for all three grasses. The opposite trend occurred with A_n (Table 4). The photosynthesis submodel, in spite of its greater complexity, did not fit the data as well as the conductance submodel. Linking the stomatal submodel with a photosynthesis submodel does allow conductance to be simulated solely from environmental conditions, but simulations are subject to the same variability as simulated photosynthesis.

The greatest source of random error in the integrated model appears to be leaf-to-leaf variability, particularly in the photosynthesis submodel. The data used in model development included treatments on individual leaves. Error analyses on model residuals reveal that the leaf-to-leaf variation accounts for a greater portion of the residuals than any other factor considered. These results appear to be consistent with variation among leaves in photosynthetic capacity. It seems likely that much inter-leaf variability can be described with

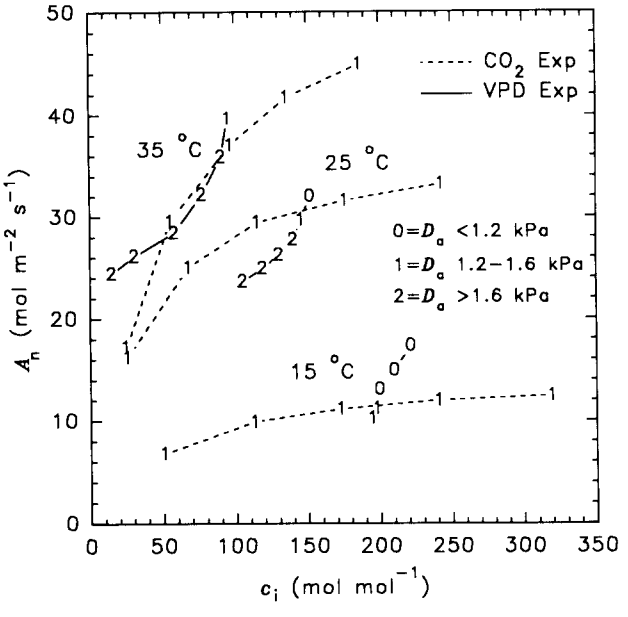

Fig. 5. Net photosynthesis measured for caucasian bluestem, plotted against leaf internal CO_2 partial pressure. Observations were made at three temperatures in two separate experiments. The first experiment included manipulations of c_a at constant D_a; in the second, D_a was manipulated at constant c_a. Each point represents the average measurements of five to eight leaves; points connected by a line represent a single group of leaves exposed to either a D_a or a c_a treatment. Numbers at a point indicate the average D_a for that group of leaves. Results indicate either a nonstomatal effect of humidity on photosynthesis, or systematic errors in estimation of c_i. Data are from Coyne and Bradford (1985).

the parameter pair K_a and E_a in the photosynthesis submodel, used to calculate A_m. Conceptually, these can be described as representing concentration of nitrogen or enzymes, which are known to limit photosynthetic rates (Boot and den Dubbelden, 1990).

5.3. *Possible importance of heterogeneous stomatal closure*

A further source of variability in the leaf model is revealed in the response of the integrated model to D_a (Fig. 3), where simulated A_n is relatively constant compared with the observed values, especially at low temperatures. The observed decreases in A_n with increasing D_a are not explained by any of the environmental variables included in the photosynthesis submodel· temperature and light were constant during this experiment, and observed c_i decreased only slightly (Fig. 5). More complete photosynthesis submodels, e.g. Farquhar et al. (1980) and Collatz et al. (1991), use the same variables as in the model used here, and are also unable to fit these humidity effects.

One plausible explanation for the discrepancy in A_n/c_i relationships

between the c_a and the D_a treatments (Fig. 5) is systematic error in the estimation of c_i in the original experiments. Such systematic errors have recently been attributed to heterogeneous stomatal closure (Van Kraalingen, 1990; Terashima, 1992), as have apparently nonstomatal reductions in photosynthesis (Downton et al., 1988). Grass leaves seem likely to exhibit variable gas exchange across their width, because of the division of photosynthetic tissue into parallel 'pipes' separated by extensions of vascular tissue (Van Kraalingen, 1990; Terashima, 1992). During periods of high vapor pressure deficit and rapid transpiration, heterogeneous stomatal closure may develop in grass leaves as water stress increases in individual pipes served by relatively inefficient xylem veins. Local variations in boundary layer conductance (Nobel, 1991, p. 364) may contribute further to this phenomenon. When substantial portions of a leaf are inactive because of local stomatal closure, the leaf's average c_i is likely to be overestimated (Downton et al., 1988).

Simple gas exchange models can be readily adapted to include effects of heterogeneous leaf activity, as demonstrated by Cheeseman (1991). However, the present model, which considers the effects of a leaf boundary layer on gas exchange, as well as the influence of A_n on g_S, would be more difficult to adapt. The computational burden of considering interactions among leaf regions through boundary layer effects would be large. Adopting the assumption of homogenous concentrations of gases within a leaf's boundary layer would partially reduce this burden, but would still require multiple iterations of the integrated model, which itself contains iterative solutions. Cheeseman (1991) used Monte Carlo methods to generate distributions of stomatal activity; this required hundreds of randomly generated values of g_S when the variance of g_S was large. More efficient methods such as Gauss–Legendre quadrature (Press et al., 1989) could be used to solve the integrated model over a defined distribution of the parameter b_0 (Eq. 6), much as is commonly performed for individual leaves over irradiance distributions (e.g. Goudriaan, 1986). Besides the problems of implementation, conceptual difficulties remain: it is not clear just which environmental or physiological variables cause variability in stomatal activity. Although the current study suggests that atmospheric water vapor deficit may induce heterogeneous stomatal closure, whole leaf gas exchange experiments are insufficient for determining the causes of stomatal variability (Terashima 1992). Whole leaf experiments could be used to develop correlative relationships between environmental variables and some relative indicator of leaf patchiness, but this would require more highly factorial experimental designs than those used in the present study.

5.4. Incorporating effects of water stress

Our model was developed from data on well-watered plants. Leaf water

potentials, measured after treatment, were all above −1.2 MPa, and no strong relationship with g_S or A_n was displayed in this range. Effects of leaf water potential were therefore not included in the current model. Further development of the model for use in field situations will include an effect of water potential on g_S. Field measurements of gas exchange in caucasian bluestem indicate near-complete stomatal closure at xylem water potentials of approximately −3.5 MPa (unpublished data). Preliminary analyses suggest that an additional multiplicative term in Eq. (6), similar to Jarvis' (1976) threshold equation, will adequately account for the effect of leaf water potential on both g_S and A_n.

5.5. Conclusions

The conductance model developed in this paper is applicable to three C-4 grasses measured over a wide range of environmental conditions. The model is relatively simple and easily applied. The model is empirical and does not explain mechanics of stomatal response, but its development has identified important relationships among environmental and physiological variables that may contribute to explanatory models.

The integrated gas exchange model explains environmental responses of g_S, E and A_n quite well. It also applies, with moderate loss of accuracy, for a validation data set. Precision of the model would be enhanced by additional parameters that represent physiological causes of leaf-to-leaf variability in photosynthetic capacity.

The gas exchange model allows the comparison of responses of different grasses to numerous combinations of environmental variables, based on data collected at representative values of those conditions. Such an approach allows exploration of the differences among accessions that would be expected at combinations of environmental conditions not included in the original experiments. While such explorations should be performed cautiously, the success of the integrated model at fitting its calibration data suggests that its predictions outside the range of these observations can be regarded as useful hypotheses.

Acknowledgments

We thank Drs Jeffrey Amthor, William Berg and H. Wayne Polley, and two anonymous reviewers, for helpful reviews of this manuscript.

References

Aphalo, P.J. and Jarvis, P.G., 1991. Do stomata respond to relative humidity? Plant Cell Environ., 14: 127–132.

Bakker, J.C., 1991. Leaf conductance of four glasshouse vegetable crops as affected by air humidity. Agric. For. Meteorol., 55: 23–36.

Ball, J.T., 1987. Calculations related to gas exchange. In: E. Zieger, G.D. Farquhar and I.R. Cowan (Editors), Stomatal Function. Stanford University Press, Stanford, CA, pp. 446–476.

Ball, J.T., 1988. An analysis of stomatal conductance. PhD Dissertation, Stanford University, CA, 89 pp.

Boot, R.G.A. and den Dubbelden, K.C., 1990. Effects of nitrogen supply on growth, allocation and gas exchange characteristics of two perennial grasses from inland dunes. Oecologia, 85: 115–121.

Bunce, J.A., 1987. In-phase cycling of photosynthesis and conductance at saturating carbon dioxide pressure induced by increases in water vapour pressure deficit. J. Exp. Bot., 38: 1413–1420.

Cheeseman, J.M., 1991. PATCHY: simulating and visualizing the effects of stomatal patchiness on photosynthetic CO_2 exchange studies. Plant Cell Environ., 14: 593–599.

Collatz, G.J., Ball, J.T., Grivet, C. and Berry, J.A., 1991. Physiological and environmental regulation of stomatal conductance, photosynthesis and transpiration: a model that includes a laminar boundary layer. Agric. For. Meteorol., 54: 107–136.

Coyne, P.I. and Bradford, J.A., 1983. Leafgas exchange in 'Caucasian' bluestem in relation to light, temperature, humidity, and CO_2. Agron. J., 76: 107–113.

Coyne, P.I. and Bradford, J.A., 1985. Comparison of leaf gas exchange and water-use efficiency in two eastern gamagrass accessions. Crop Sci., 25: 65–75.

Coyne, P.I., Bradford, J.A. and Dewald, C.L., 1982. Leaf water relations and gas exchange in relation to forage production in four Asiatic bluestems. Crop Sci., 22: 1036–1040.

Downton, W.J.S., Loveys, B.R. and Grant, W.J.R., 1988. Non-uniform stomatal closure induced by water stress causes putative non-stomatal inhibition of photosynthesis. New Phytol., 110: 503–509.

Draper, N.R. and Smith, H., 1981. Applied Regression Analysis, 2nd edition. Wiley, New York, 709 pp.

Farquhar, G.D. and Wong, S.C., 1984. An empirical model of stomatal conductance. Aust. J. Plant Physiol., 11: 191–210.

Farquhar, G.D., von Caemmerer, S. and Berry, J.A., 1980. A biochemical model of photosynthetic CO_2 assimilation in leaves of C3 plants. Planta, 149: 78–90.

Feng, Y., Li, X. and Boersma, L., 1990. The Arrhenius function as a model for explaining plant responses to temperature and water stress. Ann. Bot., 66: 237–244.

Field, C.B., Ball, J.T. and Berry, J.A. 1989. Photosynthesis: principles and field techniques. In: R.W. Pearcy, J.R. Ehleringer, H.A. Mooney and P.W. Rundel (Editors), Plant Physiological Ecology: Field Methods and Instrumentation. Chapman and Hall, London, pp. 209–253.

Goudriaan, J., 1986. A simple and fast numerical method for the computation of daily totals of crop photosynthesis. Agric. For. Meteorol., 38: 249–254.

Jarvis, P.G., 1976. The interpretations of the variations in leaf water potential and stomatal conductance found in canopies in the field. Philos. Trans. R. Soc. London (Ser. B), 273: 593–610.

Karlsson, P.E. and Assman, S.M., 1990. Rapid and specific modulation of stomatal conductance by blue light in ivy (*Hedera helix*). Plant Physiol., 94: 440–447.

Leuning, R., 1990. Modelling stomatal behaviour and photosynthesis of *Eucalyptus grandis*. Aust. J. Plant Physiol., 17: 159–175.

Losch, R. and Tenhunen, J.D., 1981. Stomatal responses to humidity—phenomenon and mechanism. In: P.G. Jarvis and T.A. Mansfield (Editors), Stomatal Physiology. Society for Experimental Biology Seminar Series, vol. 8. Cambridge University Press, Cambridge, pp. 137–161.

Mott, K.A., 1988. Do stomata respond to CO_2 concentrations other than intercellular? Plant Physiol., 86: 200–203.

Mott, K.A. and Parkhurst, D.F., 1991. Stomatal responses to humidity in air and helox. Plant Cell Environ., 14: 509–515.

Nobel, P.S., 1991. Physiochemical and Environmental Plant Physiology. Academic Press, San Diego, 635 pp.

Pearcy, R.W., Schulze, E.-D. and Zimmerman, R., 1989. Measurement of transpiration and leaf conductance. In: R.W. Pearcy, J.R. Ehleringer, H.A. Mooney and P.W. Rundel (Editors), Plant Physiological Ecology: Field Methods and Instrumentation. Chapman and Hall, London, pp. 137–160.

Press, W.H., Flannery, B.P., Teukolsky, S.A. and Vetterling, W.T., 1989. Numerical Recipes (FORTRAN Version). Cambridge University Press, Cambridge, 702 pp.

Prioul, J.L. and Chartier, P., 1977. Partitioning of transfer and carboxylation components of intracellular resistance to photosynthetic CO_2 fixation: a critical analysis of the methods used. Ann. Bot., 41: 789–800.

Radin, J.W., Hartung, W., Kimball, B.A. and Mauney, J.R., 1988. Correlation of stomatal conductance with photosynthetic capacity of cotton only in a CO_2-enriched atmosphere: mediation by abcisic acid? Plant Physiol., 88: 1058–1062.

Tenhunen, J.D. and Westin, S.S., 1979. Development of a photosynthesis model with an emphasis on ecological applications. IV. Wholephot-whole leaf photosynthesis in response to four independent variables. Oecologia, 41: 145–162.

Terashima, I., 1992. Anatomy of non-uniform leaf photosynthesis. Photosynthesis Res., 195–212.

Van Bavel, C.H.M., 1975. A behavioral equation for leaf carbon dioxide assimilation and a test of its validity. Photosynthetica, 9: 165–176.

Van Kraalingen, D.W.G., 1990. Implications of non-uniform stomatal closure on gas exchange calculations. Plant Cell Environ., 13: 1001–1004.

Wong, S.C., Cowan, I.R. and Farquhar, G.D., 1979. Stomatal conductance correlates with photosynthetic capacity. Nature, 282: 424–426.

Appendix 1. List of symbols, with definition, units and equation where defined or used in text

Symbol	Definition	Units*	Equation
A_1	photosynthetic capacity limited by light and A_m	$mol\,m^{-2}\,s^{-1}$	7
A_2	photosynthetic capacity limited by c_i and A_m	$mol\,m^{-2}\,s^{-1}$	8
A_m	maximum photosynthetic capacity	$mol\,m^{-2}\,s^{-1}$	10
A_n	net photosynthesis	$mol\,m^{-2}\,s^{-1}$	9
b_0, b_1, b_2	empirical parameters	various	1
c_a	ambient CO_2 mole fraction	$mol\,mol^{-1}$	–
c_i	leaf internal CO_2 mole fraction	$mol\,mol^{-1}$	11
c_s	leaf surface CO_2 mole fraction	$mol\,mol^{-1}$	1
dH	empirical parameter	$J\,mol^{-1}$	10
D_a	ambient saturation deficit	kPa	–
D_s	leaf surface saturation deficit	kPa	2
E	transpiration	$mol\,m^{-2}\,s^{-1}$	–
E_a	empirical parameter	$J\,mol^{-1}$	10

* Except as specified after numbers or in figures.

e_a	ambient water vapor pressure	kPa	–
E_c	CO_2 efficiency	dimensionless	8
e_s	leaf surface water vapor pressure	kPa	–
g_S	stomatal conductance to water vapor	$mol\,m^{-2}\,s^{-1}$	1
h_S	leaf surface relative humidity	fraction	1
K_a	empirical parameter determining maximum photosynthetic rate	$\ln(mol\ CO_2\,m^{-2}\,s^{-1})$	10
Q_p	photosynthetic photon flux density	$mol\,m^{-2}\,s^{-1}$	7
R_d	dark respiration	$mol\,CO_2\,m^{-2}s^{-1}$	9
T_k	leaf temperature	K	10
T_l	leaf temperature	°C	–
T_o	Optimum temperature for photosynthesis	°C	10
α	quantum efficiency	mol CO_2 mol^{-1} incident photons	7
Γ	CO_2 compensation point	$mol\,mol^{-1}$	–
θ	empirical shape parameter	dimensionless	7

Appendix 2. Goodness-of-fit statistics

The coefficient of determination (r^2) is useful for evaluating the strength of the linear relationship between variables; we use it to compare alternative linear or linearized models (e.g. Table 1). However, r^2 is less suitable for evaluating the fit of a fully specified model to data. For such purposes, we use the relative absolute mean error (RAME), defined as

$$\frac{\sum_{i=1}^{n} |y_i - \hat{y}_i|}{n \cdot y} \times 100 \qquad \text{(A1)}$$

This statistic expresses the average absolute value of the residuals as a percent of the average observed value. Unlike r^2, it measures the goodness of fit of a parameterized model. Unlike metrics such as mean square residuals, it allows comparison of models calculated from different units; because it uses absolute values instead of squared values, it does not emphasize the influence of a small number of outliers.